Synthesis of α-Willemite Nanoparticles by Post-calcination of Flame-made Zinc Oxide/Silica Composites

Takao Tani*, Lutz Mädler, Sotiris E. Pratsinis****

(Received: 19 March 2002; accepted: 22 August 2002)

Abstract

Composite ZnO/SiO_2 nanoparticles were made by flame spray pyrolysis (FSP). Characteristics of the product powder and its crystallization behavior on post-calcination were evaluated. Polyhedral aggregates of nano-sized primary particles consisting of ZnO nanocrystals 1 – 3 nm in size and amorphous SiO_2 were obtained by FSP. A short residence time in the flame can result in the co-existence of the ZnO and SiO_2 clusters without substitution or reaction hindering each other's grain growth. There was almost no change in the XRD pattern by calcination at 600 °C for 2 h, suggesting a high thermal stability of the ZnO nanocrystals in the composite particles. A pure α-willemite phase was obtained at 900 °C. At this calcination temperature, d_C and d_{BET} of the powder were 63 and 44 nm, respectively. The nano-composite structure of the FSP-made particles can suppress crystalline growth of ZnO during calcination to maintain a high reactivity of ZnO with SiO_2, obtaining pure α-willemite with high specific surface area at low calcination temperatures.

Keywords: flame spray pyrolysis, nano-composite particles, silica, willemite, zinc oxide

1 Introduction

Mn-doped rhombohedral zinc silicate (Zn_2SiO_4: α-willemite) has been used widely as a green phosphor material for plasma display panels (PDP) [1]. The α-willemite phase is produced typically by solid-state synthesis at high temperatures (e. g. 1200 °C) and milling after calcination [2, 3]. In order to prevent degradation of its luminescence properties by the milling process, emphasis is placed on developing alternative routes to fine α-willemite particles.

Li et al. [4] investigated α-willemite particle synthesis by hydrothermal processing where they controlled the particle morphology (cubic or acicular) and diameter from 200 to 1500 nm by adjusting the hydrothermal conditions. Lu et al. [5] produced α-willemite particles 350 – 700 nm in diameter by seeded hydrothermal synthesis. Zhang et al. [6] made α-willemite particles of 40 – 100 nm diameter with a small amount of triclinic zinc silicate by sol-gel synthesis and post-calcination at 850 °C. Morimo et al. [7] obtained α-willemite particles 1000 – 6000 nm in diameter by spray pyrolysis (SP) and post-calcination at 1100 °C. Kang and Park [8] examined α-willemite particle synthesis by SP at various synthesis (furnace) and post-calcination temperatures. They reported that SP at 1000 °C resulted in a mixed phase of ZnO and orthorhombic zinc silicate (β-willemite) while post-calcination at 800 °C initiated formation of α-willemite and at 1200 °C a pure α-willemite phase was obtained. Lenggoro et al. [2] successfully prepared α-willemite particles 300 and 50 nm diameter and crystalline size, respectively, by SP without post-calcination. This was achieved by applying a high temperature (1300 °C) and long residence time ($\sim$ 4 s) during the SP process. Other methods for zinc silicate synthesis are wet chemical synthesis [3], combustion synthesis and post-calcination [9] and low-temperature synthesis in an aqueous medium [10].

In summary, the reported α-willemite particles ranged from several hundred nanometers to several micrometers in size. This may be caused by the fact that the particle size demanded for a PDP-phosphor today is several micrometers (e. g. 1 – 4 μm [1]) and a high temperature is necessary to obtain pure α-willemite except for the hydrothermal method. The applied high

* *T. Tani*, Toyota Central R & D Labs., Inc., Nagakute, Aichi 480-1192 (Japan).

** Dr. *L. Mädler*, Prof. Dr. *S. E. Pratsinis* (corresponding author), Particle Technology Laboratory, Department of Mechanical and Process Engineering, ETH Zürich, Sonneggstrasse 3, 8092 Zürich (Switzerland).
E-mail: pratsinis@ivuk.mavt.ethz.ch

 0934-0866/02/0511-0354 $ 17.50+.50/0

temperature always resulted in a crystalline growth. On the other hand, nano-crystalline phosphor materials of less than 10 nm in crystalline size have attracted attention owing to their high luminescent efficiency as observed in Tb-doped Y_2O_3 [11, 12]. Therefore, it is important to establish a process for controlled nano-crystalline α-willemite synthesis, considering existing and future demands on particle size.

Flame synthesis [13] is one of the established commercial processes for making inexpensive ceramic nanoparticles. Especially flame spray pyrolysis (FSP) [14, 15], in which liquid precursor solutions are used, is a promising technique because a broad variety of precursors are available for powder synthesis. This study was focused on the synthesis of α-willemite nanoparticles by post-calcination of FSP-made ZnO/SiO_2 nano-composite particles.

2 Experimental

Zinc acrylate (ZA) (Fluka, 98%) and hexamethyldisiloxane (HMDSO) (Fluka, 99%) were used as Zn and Si sources, respectively. A mixture of 94 vol.% methanol (J. T. Baker, exceed ACS grade) and 6 vol.% acetic acid (Scharlau, reagent grade) was used as solvent. Stoichiometric ZA and HMDSO (Zn : Si = 2 : 1 molar ratio) were mixed with the solvent and stirred ultrasonically to obtain a transparent solution with a total metal (Zn + Si) concentration of 0.5 mol/l. Powder synthesis was carried out using a spray flame reactor [15, 16]. A glass syringe supplied 2 ml/min precursor solution into a nozzle, where the precursor solution was dispersed into droplets by a 3.85 l/min oxygen flow. The spray was ignited by 18 surrounding supporting flamelets, in which the total flow rates of methane and oxygen were 1.58 and 1.52 l/min, respectively. In addition, 9.8 l/min of oxygen sheath gas surrounding the nozzle was supplied to provide an excess of oxidant for complete reaction. The FSP-made powder was collected with the aid of a vacuum pump on a glass-fiber filter (Whatman, GF/A, 150 mm in diameter). The collected powder was calcined in an alumina crucible at 600, 800, 850, 900 and 1000 °C for 2 h in air applying a heating rate of 5 °C/min (Carbolite, CWF 13/23).

The particle morphology was observed by transmission electron microscopy (TEM) (Hitachi, H600, 100 kV) and high-resolution TEM (HR-TEM) (Philips, CM30ST, 300 kV). The crystalline phase of the powder was measured by X-ray diffraction (XRD) (Bruker, AXS D8 Advance, 40 kV, 40 mA) at 2θ(Cu Kα) = 20 – 70 °. The crystalline size (d_C) of α-willemite prepared by post-calcination was calculated from the full width at half-maximum (FWHM) of the (– 220) peak using Scherrer's equation [17]. The peak broadening caused by the equipment was determined as 0.131° by measuring the FWHM of the (– 220) peak using α-willemite particles several microns in diameter. The specific surface area (SSA) of the powder was measured by five-point nitrogen adsorption (BET: Micromeritics, Gemini 2350) after degassing the powder at 150 °C for 2 h in nitrogen. The BET-equivalent average primary particle diameter (d_{BET}) was calculated from the measured SSA and a density of the powder. For α-willemite, the density of $4.1 \cdot 10^3$ kg/m^3 [18] was used for the calculation. In the case of the FSP-made composite powder, the density was determined as $4.5 \cdot 10^3$ kg/m^3, assuming that the density is described as the sum of two-thirds of the ZnO density and one-third of the SiO_2 density.

3 Results and Discussion

3.1 Characteristics of the FSP-made Powder

Figure 1a shows a TEM picture of the FSP-made particles, which are polyhedral aggregates of primary particles, as typically observed with vapor flame-made SiO_2 and TiO_2 [13]. Because of the similarity in particle morphology of vapor flame and spray flame-made particles, it can be inferred that the FSP-made particles were formed in the gas phase. Figure 1b shows a detailed structure of the primary particles (HR-TEM picture). The primary particles consisted of fine crystal domains 1 – 3 nm in size and amorphous phase. The observed lattice distance of the crystals (Figure 1b) was 0.163 nm, which is in agreement with the distances of the (110) plane (0.162 nm) in hexagonal ZnO (zincite, #36-1451) and the (02 15) plane (0.164 nm) in β-willemite (#14-0653).

Figure 2 shows a XRD pattern of the as-prepared powder and the peak positions of zincite.

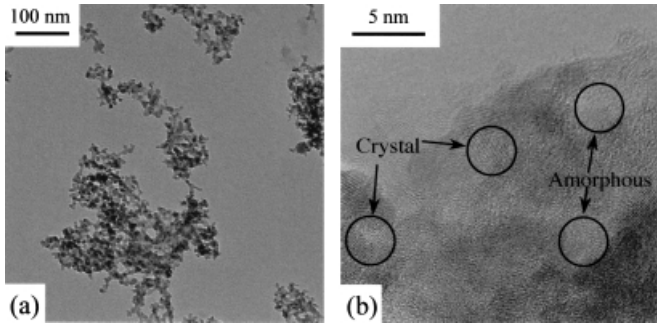

Fig. 1: Morphology of the FSP-made particles by transmission electron microscopy (TEM) (a) and detailed structure of the primary particles by high-resolution TEM (b). The primary particles consisted nano-crystals of 1 – 3 nm in size and amorphous phase.

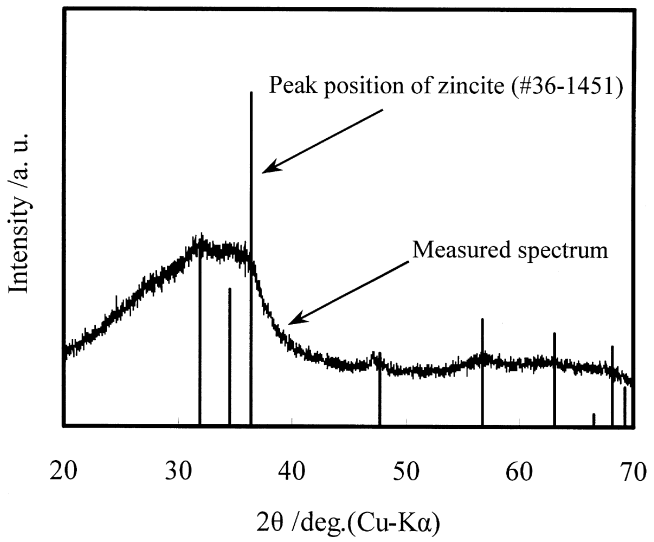

Fig. 2: X-ray diffraction pattern of the FSP-made powder and the peak positions of zincite. Diffused peaks are observed at the same positions as those of zincite.

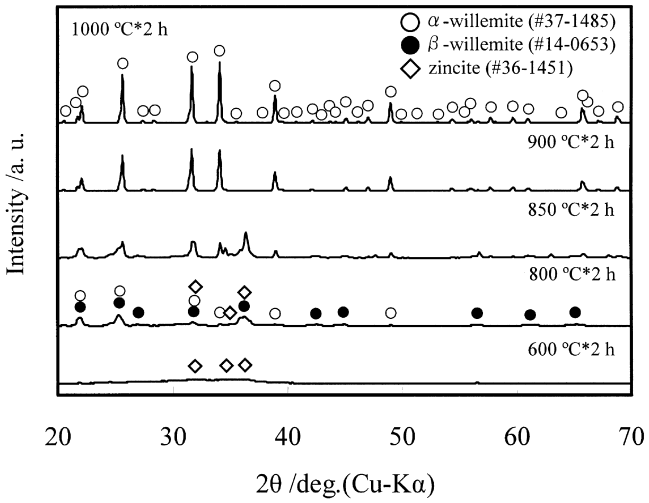

Fig. 3: Change of the X-ray diffraction (XRD) pattern by post-calcination of the FSP-made powder. There is almost no change in the XRD spectra until 600 °C. A pure α-willemite phase is obtained after calcination at 900 °C.

The peaks were observed at the same positions as those of zincite, although they were diffused. A peak of willemite at $\sim 25^\circ$ was not detected. The SSA was 162 m^2/g, giving an average primary particle diameter of 8.2 nm, which qualitatively corresponded to the observed primary particles of the mixed oxides in the TEM (Figure 1a). According to the HR-TEM observations and a detailed evaluation of the XRD data reported earlier [16], the primary particles were regarded as a composite, in which ZnO crystals of 1 – 3 nm in size were dispersed in/on amorphous SiO_2. The β-willemite (Zn_2SiO_4) phase is formed at 722 °C from sol-gel derived amorphous zinc silicate [19]. Although the flame temperature is far higher than that, the crystallization of zinc silicates may be difficult at residence times of the order of milliseconds within the hot spray flame, resulting in a state where the ZnO and SiO_2 clusters coexist without substitution or reaction but hindering each other's grain growth.

3.2 Formation of α-Willemite by Post-Calcination

Figure 3 shows the change in the XRD pattern of the FSP-made powder after post-calcination. There was almost no difference in the XRD pattern on calcination at 600 °C for 2 h, suggesting that the dispersed ZnO nanocrystals in the composite particles were stabilized by the amorphous SiO_2 phase without the reaction between ZnO and SiO_2. Crystallization of β-willemite was observed by calcination at 800 °C. The formation of β-willemite was reported also by Kang and Park [8] and Lenggoro et al. [2] at low furnace temperatures ($< \sim 1000$ °C) in SP, suggesting that β-willemite is an intermediate phase before forming α-willemite. Nucleation of α-willemite (#37-1485) as well as a slight crystalline growth of ZnO were observed at a calcination temperature of 850 °C. The formation of pure α-willemite and its crystalline growth occurred on calcination at 900 and 1000 °C, respectively. The observed FWHM values were 0.260 and 0.226 °, giving d_C of 63 and 85 nm for the calcined powders at 900 and 1000 °C, respectively. The d_{BET} values were 44 and 77 nm for the calcined powders at 900 and 1000 °C, respectively, which were slightly smaller than d_C. This may be caused by an inhomogeneous particle size distribution and/or non-smooth particle surface. If large particles are contained in the powder, they may have little influence on the specific surface area but can sharpen the XRD peaks, resulting in larger d_C than d_{BET}. On the other hand, a non-smooth particle surface can increase the SSA, also resulting in larger d_C than d_{BET}.

Figure 4 shows the TEM micrographs of α-willemite particles after calcination at 900 and 1000 °C. The primary particles were nearly spherical and partially aggregated (or necked). The observed primary particle diameters were qualitatively consistent with the d_C of the corresponding particles, indicating that the primary particles were single crystalline.

The BET-equivalent average primary particle diameters of the α-willemite powders produced in this study were lower than those of the direct SP-made particles (300 nm) [2] and equivalent to those of (sol-gel synthesis + post-calcination)-made particles (40 – 100 nm) [6]. The d_C in this study was equivalent to that of the direct SP-made particles (~ 50 nm) [2]. For the FSP-made powder, the

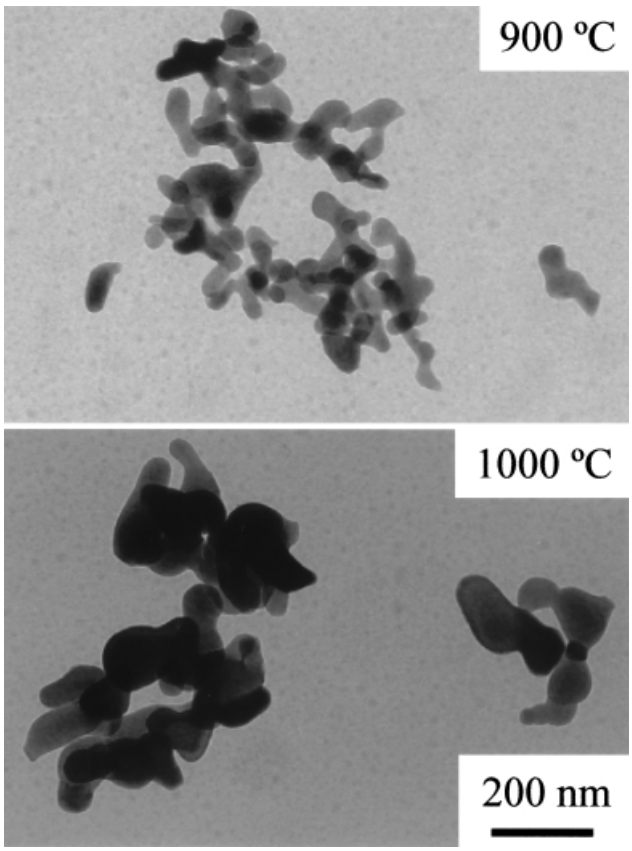

Fig. 4: Transmission electron microscopic images of the α-willemite particles obtained after calcination for 2 h at 900 and 1000 °C.

temperature of pure α-willemite formation (900 °C) was much lower than that for SP [8], where the diffraction peaks of ZnO still remained after post-calcination at 1000 °C, although the nucleation temperature of α-willemite was higher in the FSP-made powder (850 °C) than that of the SP-made powder (800 °C) [8].

The ZnO crystals in the as-prepared FSP-made powder are considered highly crystalline and thus thermally stable because of the high reaction temperature in the spray flame, which may suppress the crystallization of α-willemite at a low calcination temperature (800 °C). On the other hand, once large ZnO particles are formed, they can sustain high temperatures (e.g. 1000 °C) because large ZnO particles may be less reactive with SiO_2, disturbing pure α-willemite formation. However, in the FSP-made powder, crystalline growth of ZnO can be suppressed during calcination by SiO_2 [20, 21], thus, maintaining, a small ZnO size and hence high reactivity for these crystals, resulting in a pure α-willemite formation with less particle growth at lower calcination temperatures. The α-willemite powder obtained by post-calcination of the FSP-made powder is one of the smallest in both primary particle diameter and crystalline size, which may make it promising as a phosphor material.

4 Conclusion

Polyhedral aggregates of ZnO/SiO_2 composite nanoparticles were made by FSP. The primary particles consisted of ZnO nano-crystals 1 – 3 nm in size and amorphous SiO_2. The d_{BET} was 8.2 nm, which is in agreement with the observed diameter in TEM. A short residence time in the hot zone (spray flame) can result in the co-existence of the ZnO and SiO_2 clusters without substitution or reaction hindering each other's grain growth. There was almost no change in the XRD pattern by calcination at 600 °C for 2 h, suggesting that the dispersed ZnO nano-crystals in the composite particles were stabilized by the amorphous SiO_2 phase without a reaction between ZnO and SiO_2. Crystallization of β-willemite and nucleation of α-willemite as well as slight crystalline growth of ZnO were observed by calcination at 800 and 850 °C, respectively. A pure α-willemite phase was obtained at a calcination temperature of 900 °C. The d_C and d_{BET} values of the calcined powders were 63 and 44 nm at 900 °C and 85 and 77 nm at 1000 °C, respectively, which were qualitatively consistent with the observed diameters in TEM. These values are among the smallest reported in the literature. The nano-composite structure of the FSP-made particles can suppress the crystalline growth of ZnO during calcination to maintain a high reactivity of ZnO with SiO_2, achieving pure α-willemite formation at lower calcination temperatures than with other processes.

5 Acknowledgements

The authors are grateful to Dr. Frank Krumeich (ETHZ) and Dr. Martin Müller (ETHZ) for the HR-TEM observations and providing the TEM equipment, respectively. This research was carried out at the Institute of Process Engineering of ETH Zürich under the foundation of Toyota Central R&D Labs., Inc. and the Kommission für Technologie und Innovation (KTI) TOP NANO 21, grant #5351.1, Switzerland.

6 Symbols and Abbreviations

d_{BET}	nm	BET-equivalent average primary particle diameter
d_C	nm	crystalline size calculated using Scherrer's equation
FSP		flame spray pyrolysis

FWHM full width at half-maximum
HR – TEM high-resolution transmission electron microscopy
SP spray pyrolysis
SSA specific surface area
TEM transmission electron microscopy
XRD X-ray diffraction

7 References

[1] T. Justel, H. Nikol, Optimization of luminescent materials for plasma display panels. *Adv. Mater.*, **2000**, *12*, 527 – 530.

[2] I. W. Lenggoro, F. Iskandar, H. Mizushima, B. Xia, K. Okuyama, N. Kijima, One-step synthesis for Zn_2SiO_4: Mn particles 0.3 – 1.3 μm in size with spherical morphology and non-aggregation. *Jpn. J. Appl. Phys. Part 2 – Lett.*, **2000**, *39*, L1051 – L1053.

[3] I. F. Chang, J. W. Brownlow, T. I. Sun, J. S. Wilson, Refinement of zinc silicate phosphor synthesis. *J. Electrochem. Soc.*, **1989**, *136*, 3532 – 3536.

[4] Q. H. Li, S. Komarneni, R. Roy, Control of morphology of Zn_2SiO_4 by hydrothermal preparation. *J. Mater. Sci.*, **1995**, *30*, 2358 – 2363.

[5] S. W. Lu, T. Copeland, B. I. Lee, W. Tong, B. K. Wagner, W. Park, F. Zhang, Synthesis and luminescent properties of Mn^{2+} doped Zn_2SiO_4 phosphors by a hydrothermal method. *J. Phys. Chem. Solids*, **2001**, *62*, 777 – 781.

[6] H. X. Zhang, S. Buddhudu, C. H. Kam, Y. Zhou, Y. L. Lam, K. S. Wong, B. S. Ooi, S. L. Ng, W. X. Que, Luminescence of Eu^{3+} and Tb^{3+} doped Zn_2SiO_4 nanometer powder phosphors. *Mater. Chem. Phys.*, **2001**, *68*, 31 – 35.

[7] R. Morimo, R. Mochinaga, K. Nakamura, Preparation and characterization of a manganese activated zinc silicate phosphor by fume pyrolysis of an alkoxide solution [Zn_2SiO_4_Mn]. *Mater. Res. Bull.*, **1994**, *29*, 751 – 757.

[8] Y. C. Kang, S. B. Park, Zn_2SiO_4: Mn phosphor particles prepared by spray pyrolysis using a filter expansion aerosol generator. *Mater. Res. Bull.*, **2000**, *35*, 1143 – 1151.

[9] G. T. Chandrappa, S. Ghosh, K. C. Patil, Synthesis and properties of willemite Zn_2SiO_4 and M^{2+}: Zn_2SiO_4 (M = Co and Ni). *J. Mater. Synth. Process*, **1999**, *7*, 273 – 279.

[10] T. S. Ahmadi, M. Haase, H. Weller, Low-temperature synthesis of pure and Mn-doped willemite phosphor (Zn_2SiO_4: Mn) in aqueous medium. *Mater. Res. Bull.*, **2000**, *35*, 1869 – 1879.

[11] R. N. Bhargava, The role of impurity in doped nanocrystals. *J. Lumin.*, **1997**, *72 – 4*, 46 – 48.

[12] E. T. Goldburt, B. Kulkarni, R. N. Bhargava, J. Taylor, M. Libera, Size dependent efficiency in Tb doped Y_2O_3 nanocrystalline phosphor. *J. Lumin.*, **1997**, *72 – 4*, 190 – 192.

[13] S. E. Pratsinis, Flame aerosol synthesis of ceramic powders. *Prog. Energy Combust. Sci.*, **1998**, *24*, 197 – 219.

[14] M. Sokolowski, A. Sokolowska, A. Michalski, B. Gokieli, The "in-flame-reaction" method for Al_2O_3 aerosol formation. *J. Aerosol Sci.*, **1977**, *8*, 219 – 230.

[15] L. Mädler, H. K. Kammler, R. Mueller, S. E. Pratsinis, Controlled synthesis of nanostructured particles by flame spray pyrolysis. *J. Aerosol Sci.*, **2002**, *33*, 369 – 389.

[16] T. Tani, L. Mädler, S. E. Pratsinis, Zinc oxide/silica composite nanoparticle synthesis by flame spray pyrolysis. *J. Mater. Sci.*, **2002**, in press.

[17] H. P. Klug, L. E. Alexander, *X-ray Diffraction Procedures.* John Wiley & Sons, New York, **1974.**

[18] D. R. Lide, *CRC Handbook of Chemistry and Physics, 81st edition*. CRC Press, Boca Raton, FL, **2000.**

[19] C. C. Lin, P. Y. Shen, Nonisothermal site saturation during transformations of Zn_2SiO_4. *J. Solid State Chem.*, **1994**, *112*, 387 – 391.

[20] M. K. Akhtar, S. E. Pratsinis, S. V. R. Mastrangelo, Dopants in vapor-phase synthesis of titania powders. *J. Am. Ceram. Soc.,* **1992**, *75*, 3408 – 3416.

[21] S. Vemury, S. E. Pratsinis, Dopants in flame synthesis of titania. *J. Am. Ceram. Soc.*, **1995**, *78*, 2984 – 2992.